Preparation and Performance Evaluation of Valonia Tannin-sucrose Wood Adhesive Based on Sucrose Proportion Regulation

Ningyuan Zuo,[a,#] Wenjun Zhao,[a,#] Guorong Xie,[b] Jinye Zhou,[a] Qiuli Li,[a] Huali Li,[a] Chuchu Chen,[a] Tong Meng,[a] and Zhigang Wu [a,*]

Valonia tannin, a typical hydrolysable tannin, was used as the raw material and sucrose as the cross-linking agent to investigate the influence of sucrose proportion on the structure and performance of the adhesive. The aim was to evaluate the feasibility of utilizing hydrolysable tannins for wood adhesives. Fourier transform infrared spectroscopy confirmed that valonia tannin belongs to a typical hydrolysable gallotannin, with ester bond linkages and ortho-trisubstituted benzene ring structures present in the molecule. The bonding performance results showed that as the sucrose proportion increased from 66.7% to 100%, the dry strength increased from 1.04 to 1.43 MPa, and the warm-water strength increased from 0.46 to 0.84 MPa, meeting the requirements for Class II plywood specified in the GB/T 17657 (2022) standard. Increasing the sucrose proportion promoted the dehydration of sucrose toward 5-hydroxymethylfurfural, which is proposed to subsequently form a dense three-dimensional cross-linked network with valonia tannin based on our group's prior condensed-tannin studies, effectively compensating for the deficiencies of hydrolysable tannins in terms of low reactivity and unstable ester bonds. This study provides a theoretical basis and experimental support for the high-value utilization of hydrolysable tannins in the field of wood adhesives.

DOI: 10.15376/biores.21.4.10676-10688

Keywords: Valonia tannin; Sucrose; Wood adhesive; Bonding performance; Thermal properties

*Contact information: a: College of Forestry, Guizhou University, Guiyang 550025, China; b: Guizhou Xusheng Wood Industry Co., Ltd., Qiandongnan 556011, China; #: These two authors contributed equally to this work; *Corresponding author: wzhigang9@163.com*

INTRODUCTION

The wood-based panel industry is a core sector for the efficient utilization of wood resources. As a key component determining the performance and environmental attributes of wood-based panels, the technological upgrading of adhesives is directly related to the green transformation of the industry. For a long time, petroleum-based synthetic adhesives, such as urea–formaldehyde and phenol–formaldehyde resins, have dominated the market due to their low cost and mature processing technology. Nevertheless, the curing and long-term application of these adhesives are accompanied by the sustained emission of hazardous compounds, notably formaldehyde, which may compromise indoor air quality and endanger human health (Wu *et al*. 2021; Li *et al*. 2023; Wang *et al*. 2023, 2024; Ma *et al*. 2024). With increasingly stringent environmental regulations, the development of formaldehyde-free, low-toxicity, and renewable biomass-based wood adhesives has become an important research direction for green manufacturing in the wood industry (Li *et al*. 2025; Liu *et al*. 2025; Lin and Catchmark 2025; Hou *et al*. 2025; Zheng *et al*. 2025;

Gong *et al*. 2026; Yang *et al*. 2026).

Tannin, as a natural polyphenolic product of plants, is regarded as an ideal substitute for traditional synthetic adhesives due to the abundant active phenolic hydroxyl groups in its molecules, which can undergo cross-linking reactions with aldehydes (Arias *et al*. 2021; Li *et al*. 2023; Oktay *et al*. 2024; Liang *et al*. 2024). Based on differences in chemical structure, tannins can be divided into two categories: condensed tannins and hydrolysable tannins. Among them, condensed tannins, such as bayberry tannin and acacia tannin, possess phloroglucinol-type structural units, where the aromatic ring reaction sites exhibit strong nucleophilicity and high reactivity toward electrophilic reagents, such as formaldehyde, resulting in dense cross-linked networks and demonstrating good application potential in the field of wood adhesives (Xiao *et al*. 2022, 2023; Liang *et al*. 2025a, 2025b). In contrast, hydrolysable tannins are more abundant in nature and have lower extraction costs, but their utilization as adhesives has long faced bottlenecks due to inherent structural constraints (Virtanen *et al*. 2020, 2021, 2022; Engström *et al*. 2022; Guo *et al*. 2024).

Sucrose, as a widely available and inexpensive natural sugar, has attracted considerable attention in the field of biomass-based adhesives in recent years. Studies have shown that sucrose can dehydrate under hot-pressing conditions to generate active cross-linking components, whose aldehyde groups can condense with the phenolic hydroxyl groups of tannins to form three-dimensional cross-linked networks. This reaction pathway does not require exogenous formaldehyde, fundamentally avoiding formaldehyde emission issues while achieving full biomass-based adhesives (Zhao and Umemura 2014, 2015; Zhao *et al*. 2015, 2020). Existing research has confirmed that the compounding of sucrose with condensed tannins can produce fully biomass-based adhesives with excellent bonding performance (Xiao *et al*. 2022, 2023; Zhao *et al*. 2020; Liang *et al*. 2025a), but systematic studies on the performance and network-structure response of hydrolysable tannin–sucrose adhesives, particularly the influence of sucrose proportion on the cross-linked network structure and adhesive layer performance, are still lacking.

Based on the above background, this study used valonia tannin, a typical hydrolysable tannin, as the raw material and sucrose as the cross-linking agent. Through regulating the mass ratio of sucrose to tannin, a series of valonia tannin–sucrose adhesives were prepared, and their bonding performance, microstructural morphology, and thermal stability were investigated. The aim of this research was to evaluate the feasibility of utilizing hydrolysable tannins for wood adhesives and to provide a theoretical basis and experimental support for broadening the raw material sources of biomass-based adhesives and promoting the high-value utilization of hydrolysable tannin resources.

EXPERIMENTAL

Materials

Valonia tannin (industrial grade) was supplied by Wuming Tannin Factory (Guangxi, China). The material, derived from the acorn cups of *Quercus macrolepis* (valonia oak), had a particle size of ~150 μm, a moisture content of 8 to 10%, and a tannin purity of ≥75%. Sucrose (99.0%), analytical grade, was purchased from Chengdu Jinshan Chemical Reagent Co., Ltd. Sodium dodecylbenzenesulfonate (SDBS, analytical grade, ≥90% purity) was purchased from Chengdu Jinshan Chemical Reagent Co., Ltd. and used directly as a dispersing agent without further treatment. Poplar veneer (Populus *spp*.,

moisture content 8 to 10%), with dimensions of 400 mm × 400 mm and a thickness of 1.5 mm, was sourced from Suqian, Jiangsu, China. Poplar wood typically comprises approximately 45 to 50% cellulose, 20 to 25% hemicellulose, 20 to 23% lignin, and 3 to 8% extractives on a dry mass basis (Tian *et al*. 2021).

Preparation of Tannin–sucrose Adhesive

Under ambient temperature conditions, 33.3 g of distilled water was added to a 250 mL round-bottom three-neck flask equipped with a mechanical stirrer (IKA RW 20 digital overhead stirrer, four-bladed propeller, 200 rpm), a mercury-in-glass thermometer (0 to 300 °C, ±1 °C), and condenser (300 mm, water-cooled). The mixture was heated to 60 °C, and a certain amount of sucrose was added. After complete dissolution, 30 g of valonia tannin was added in batches with continuous stirring until a paste-like consistency was obtained. Subsequently, 0.2 g of sodium dodecylbenzenesulfonate was added, and stirring was maintained for 5 min. On this basis, the proportion of sucrose relative to tannin was varied. When the sucrose proportions were 66.7% (20 g), 83.3% (25 g), and 100% (30 g) (based on the mass of tannin). The obtained adhesives were designated as ADH1, ADH2, and ADH3, respectively.

Preparation of Plywood and Bonding Performance Testing

Laboratory-made three-layer (3-ply) plywood was prepared. The adhesive was applied to the single side of each veneer using a manual hand roller. The spread mass per unit area was controlled at 160 g/ m^2 on a single side. The glued veneers were hand-assembled with the grain directions of adjacent plies perpendicular to each other, cold-pressed at room temperature for 10 min, and then immediately transferred to the laboratory hot press (LabPro 300 × 300 mm, maximum temperature 300 °C, maximum pressure 5 MPa, temperature control accuracy ±2 °C, pressure control accuracy ±0.05 MPa). The hot-pressing parameters were as follows: hot-pressing temperatures of 215 ℃, unit pressure of 1.5 MPa, and hot-pressing time of 1 min/mm. The bonding strength (dry strength, warm-water strength and boiling-water strength) was tested in accordance with the national standard GB/T 17657 (2022). The final reported strength was the average of 12 specimens.

Fourier Transform Infrared (FT-IR) Spectroscopy Testing

A Thermo Fisher Scientific Nicolet iS20 spectrometer (USA) was used to record spectra in the range of 4000 to 400 cm^{-1}, with a resolution of 4 cm^{-1} and 32 scans.

Thermogravimetric (TG) Testing

The cured adhesive powder was subjected to TG analysis. A Netzsch TG 209 F3 thermogravimetric analyzer (Germany) was used under a nitrogen purge (flow rate 50 mL/min), with a heating rate of 10 °C/min and a temperature range of 30 to 700 °C. All experiments were performed in triplicate.

Scanning Electron Microscopy (SEM) Testing

The cross-section of the cured adhesive layer was sputter-coated with gold using a Leica EM ACE200 sputter coater (gold target, 99.99%, sputtering current 30 mA, sputtering time 60 s, coating thickness approximately 10 nm) and then observed using a ZEISS GeminiSEM 300 scanning electron microscope (Germany) at an acceleration voltage of 5 kV and a working distance of 8 to 10 mm.

Statistical Analysis

Data processing and statistical analysis were performed using Microsoft Excel 2021 and Origin 2024. Specifically, raw data were collated and descriptive statistics (including mean and standard deviation) were calculated in Excel, whereas data visualization and inferential statistical analyses were conducted in Origin. One-way analysis of variance (ANOVA) was employed to assess the statistical significance of differences among multiple group means. Where ANOVA indicated a significant overall effect ($p < 0.05$), pairwise comparisons between groups were further examined using Tukey's post-hoc test. All results are expressed as mean ± standard deviation (SD), and the error bars depicted in the graphical representations denote the standard deviation derived from independent replicate measurements ($n \geq 3$).

RESULTS AND DISCUSSION

Structural Analysis of Valonia Tannin

Figure 1 presents the FT-IR spectrum of valonia tannin. Compared with condensed tannins, its spectral characteristics exhibited significant differences in molecular connection modes, benzene ring substitution patterns, and reactivity, displaying typical structural features of hydrolysable tannins.

A strong absorbance peak appeared at 1725.6 cm^{-1}, corresponding to the stretching vibration of the galloyl ester carbonyl group. Valonia tannin belongs to gallotannins, and its structure consists of multiple gallic acid units connected to a central skeleton *via* ester bonds. This peak directly confirmed the existence of ester bond structures and serves as a key marker for distinguishing hydrolysable tannins from condensed tannins (Virtanen *et al*. 2020, 2021, 2022).

The absorptions at 1613.1 cm^{-1} and 1449.0 cm^{-1} corresponded to the C=C stretching vibrations of the benzene ring skeleton, while the peak at 1340.6 cm^{-1} was attributed to the in-plane bending vibration of the phenolic hydroxyl O–H, indicating that valonia tannin is rich in phenolic hydroxyl groups and aromatic structures. The 1613.1 cm^{-1} peak position of valonia tannin was influenced by the conjugation effect of the ester carbonyl group, whereas the benzene ring skeleton vibrations of condensed tannins typically appeared as multiple peaks (Liang *et al*. 2025a). The absorbances at 1195.3 cm^{-1} and 1035.3 cm^{-1} correspond to the stretching vibrations of ester bonds, reflecting the ester linkage mode between gallic acid units and the central skeleton. Owing to this connection mode, the valonia tannin molecule adopts a radial configuration characterized by pronounced steric hindrance, which effectively blocks aldehyde molecules from approaching every reaction site. In contrast, bayberry tannin and acacia tannin exhibit aromatic ether bond absorptions at similar positions, with their molecular chains presenting linear or branched morphologies that facilitate full contact and cross-linking with aldehyde molecules (Liang *et al*. 2025b).

The absorption peak at 758.7 cm^{-1} corresponded to the out-of-plane bending vibration of the ortho-trisubstituted benzene ring in the gallic acid structural units, indicating that the phenolic hydroxyl groups of valonia tannin are distributed in a 1,2,3-ortho pattern. In contrast, the A rings of bayberry tannin and acacia tannin are of the phloroglucinol-type structure, with a meta-substitution pattern on the benzene ring. The meta-substitution activates the C6 and C8 positions of condensed tannins through the electron-donating conjugation effect of the dual phenolic hydroxyl groups, greatly

increasing the electron cloud density and enhancing nucleophilicity, resulting in high reactivity toward electrophilic substitution reactions with formaldehyde. The ortho-substitution pattern of valonia tannin, however, leads to strong hydrogen bonding and steric hindrance between the hydroxyl groups, noticeably reducing the nucleophilic activity of the available reaction sites on the aromatic ring. This is the structural origin of its poor reactivity (Virtanen *et al*. 2022; Engström *et al*. 2022; Guo *et al*. 2024).

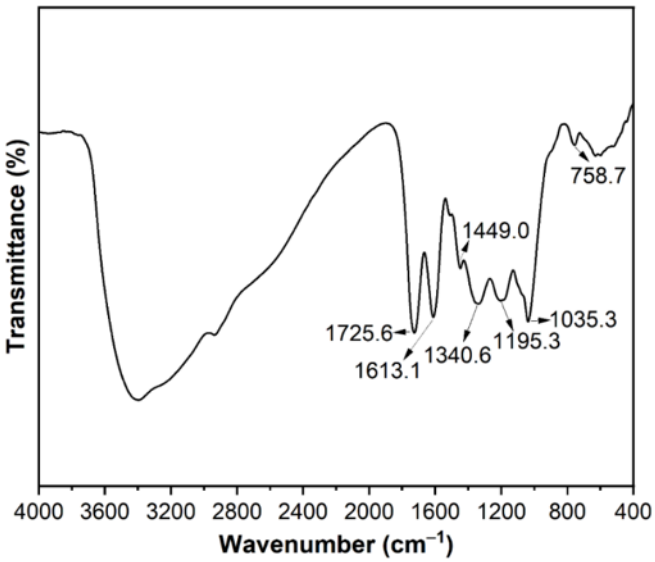

Fig. 1. FT-IR spectrum of valonia tannin

The above spectral characteristics explain the limitations of valonia tannin in wood adhesive applications. The ester bond linkages not only result in a compact molecular configuration and poor accessibility of cross-linking sites, but also render the molecule susceptible to hydrolysis or thermal cleavage during hot-pressing curing and hydrothermal aging, leading to molecular chain breakage and disintegration of the cross-linked network, with a consequent sharp decline in the cohesive strength and water resistance of the adhesive layer. Furthermore, the gallic acid units with ortho-substitution exhibit far lower reactivity than phloroglucinol-type structures, causing the cross-linking reaction efficiency of valonia tannin to be noticeably lower than that of bayberry tannin and acacia tannin, with insufficient effective cross-linking density and difficulty in forming a dense three-dimensional network.

Bonding Performance of Valonia Tannin-sucrose Adhesive

As shown in Fig. 2, as the sucrose proportion (based on tannin mass) rose from 66.7% to 100%, a gradual increase in dry strength, warm-water strength, and boiling-water strength was observed for all three adhesive formulations (ADH1, ADH2, and ADH3).

The increase in water-resistant strength was markedly higher than that of dry strength, reflecting that the sucrose dosage was crucial for the densification of the cross-linked network and the improvement of water resistance. For reference, the pure tannin adhesive exhibited merely 0.28 MPa of dry bond strength, indicating the intrinsically weak adhesion of tannin alone. By contrast, the pure sucrose adhesive achieved 0.89 MPa dry strength, 0.33 MPa warm-water strength, and 0.10 MPa boiling-water strength, demonstrating that sucrose itself possessed considerable bonding and cross-linking capability. Therefore, the progressive enhancement in adhesive strength with increasing

sucrose proportion, particularly the pronounced improvement in water resistance, further confirmed that sucrose played a dominant role in constructing a compact, water-resistant cross-linked network.

The dry strength increased from 1.04 MPa for ADH1 to 1.19 MPa for ADH2, reaching 1.43 MPa for ADH3, representing an increase of 37.5%. During hot pressing, sucrose is expected to dehydrate to generate 5-HMF. Drawing on the mechanism established for condensed tannin–sucrose adhesives (Xiao *et al.* 2022, 2023; Liang *et al.* 2025a,b), the aldehyde groups of its furan ring likely condense with the phenolic hydroxyl groups of valonia tannin to form a three-dimensional cross-linked network. The observed improvements in dry strength and water resistance are consistent with this proposed pathway, although direct spectroscopic evidence of the specific condensation adducts in the hydrolysable tannin system remains to be obtained. As the sucrose proportion increased, the yield of 5-HMF increased, the density of effective cross-linking points per unit volume increased, the intermolecular binding forces were enhanced, and the bulk strength of the adhesive layer improved. Simultaneously, the greater amount of 5-HMF improved the wetting and penetration of the adhesive on the wood surface, increasing the effective contact area and enhancing the interfacial mechanical interlocking effect, thereby leading to a steady increase in dry strength.

The variation pattern of water-resistant strength better reflected the hydrolysis resistance of the cross-linked network. The warm-water strength increased from 0.46 MPa for ADH1 to 0.67 MPa for ADH2, reaching 0.84 MPa for ADH3, representing an increase of up to 82.6%; the boiling-water strength increased from 0.38 MPa to 0.45 MPa, reaching 0.67 MPa for ADH3, an increase of 76.3%. The increase in water-resistant strength was far greater than that of dry strength, indicating that increasing the sucrose dosage contributed particularly prominently to improving the water resistance of the adhesive layer. The reason lies in the fact that the covalent cross-linking bonds formed between 5-HMF and the phenolic hydroxyl groups of tannin possess strong hydrophobicity and chemical stability. The high cross-linking density effectively reduced the number of free hydroxyl groups in the adhesive layer, thereby decreasing the adsorption and penetration sites for water molecules. In addition, the dense three-dimensional network structure physically blocked the diffusion channels of water molecules, enabling the adhesive layer to maintain high structural integrity under hot water immersion conditions. The warm-water strength of ADH3 (0.84 MPa) met the requirement for Class II plywood (not less than 0.70 MPa) specified in the GB/T 17657 (2022) standard, and it also exhibited certain boiling-water resistance, indicating that when the mass ratio of sucrose to tannin reached 100%, the cross-linking reaction was relatively sufficient and the network structure was sufficiently dense. Xiao *et al.* (2022) achieved a dry strength of 1.42 MPa and a wet strength of 0.92 MPa using bayberry tannin with sucrose under optimized hot-pressing conditions (200 °C, 1.5 MPa), while Zhao and Umemura (2014) reported a dry strength of 1.15 MPa for a tannin–sucrose particleboard adhesive. The dry strength of ADH3 (1.43 MPa) is comparable to these condensed tannin benchmarks, although its warm-water strength (0.84 MPa) was slightly lower than the best-performing condensed tannin formulations. This comparison highlights that, despite the inherent structural disadvantages of hydrolysable tannins (low reactivity, unstable ester bonds), a sufficiently high sucrose proportion can compensate to yield bonding performance that approaches the levels previously reported only for condensed tannin systems.

In summary, the sucrose dosage directly determined the yield of 5-HMF and the degree of cross-linking with tannin. Increasing the sucrose proportion evidently increased

the cross-linking density, constructed a denser and more stable network structure, and simultaneously improved both dry strength and water resistance, with particularly prominent improvement in water resistance. Although valonia tannin is a hydrolysable tannin and its ester bond linkages and ortho-substitution pattern result in lower reactivity compared with condensed tannins, when the sucrose proportion was increased to a mass ratio of 100% relative to tannin, a sufficiently dense cross-linked network could still be formed, enabling the adhesive to meet the requirements for Class II plywood and successfully achieving its application in the field of wood adhesives.

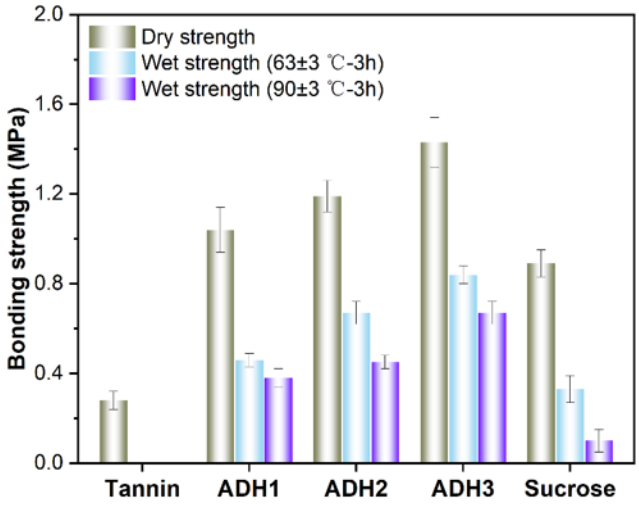

Fig. 2. The bonding strength test results of the valonia tannin-sucrose adhesive

SEM Analysis

Figure 3 shows the cross-sectional microstructural morphologies of the cured products of valonia tannin–sucrose adhesives at different sucrose proportions. The cross-section of ADH1 was relatively smooth overall, accompanied by a certain degree of cracking and small wrinkled regions. This morphological characteristic was directly related to its lower sucrose proportion. When the sucrose proportion was 66.7% relative to tannin, the amount of sucrose available for conversion to 5-HMF during hot pressing was relatively limited, and the effective cross-linking sites with the phenolic hydroxyl groups of valonia tannin failed to react sufficiently, resulting in a relatively low cross-linking density. The even surface morphology suggested that cross-linking proceeded with reasonable spatial homogeneity, yet the considerable distance between cross-linking loci, coupled with the high segmental mobility of molecular chains, resulted in a loosely constructed network after cure. Under external force or internal stress, such a low-cross-linking network could not effectively dissipate energy through local deformation, and stress tended to concentrate in weak regions, thereby inducing crack initiation and propagation, manifested as the visible cracking phenomena on the cross-section. The presence of small wrinkled regions indicated that there were still a few locally dense cross-linking regions in the system, which produced slight plastic deformation during curing shrinkage, but due to their limited proportion, their contribution to overall toughness was insufficient.

The cross-section of ADH3 presented a complex structure composed of both flat regions and wrinkled regions, with the degree of wrinkling notably increased. When the sucrose proportion was increased to 100%, the yield of 5-HMF was sufficient, and the cross-linking reaction with valonia tannin was more complete, resulting in a substantial

increase in cross-linking density. The flat regions corresponded to highly cross-linked dense networks where molecular chain segments were tightly constrained, exhibiting rigid load-bearing behavior under external force and imparting high cohesive strength to the adhesive layer. The formation of wrinkled regions originated from volume shrinkage and internal stress during the curing process under high cross-linking density. The generation of numerous cross-linking points restricted the free movement of molecular chain segments, and stress could not be uniformly released through chain slippage, instead prompting local regions to undergo wrinkling deformation. This wrinkled structure can absorb and dissipate energy through its own geometric deformation when subjected to force, reducing the degree of stress concentration and thereby imparting certain toughness characteristics to the adhesive (Liang *et al*. 2025a,b). Compared with ADH1, the proportion of wrinkled regions on the cross-section of ADH3 increased markedly, indicating that the high sucrose proportion promoted the formation of a more extensive and denser cross-linked network, enabling the adhesive layer to possess high rigidity while achieving stress buffering through the wrinkling mechanism.

However, due to the inherent limitations of the hydrolysable structure of valonia tannin, even though the cross-linking density of ADH3 had reached a relatively optimal level, the regularity and density of its wrinkled structure still lagged behind those of condensed tannin adhesives. The ortho-substitution pattern of valonia tannin exhibited low reactivity, and the ester bond linkage mode resulted in a compact molecular configuration. Although the high sucrose proportion compensated to some extent for the insufficient cross-linking sites, the thermal instability of ester bonds and steric hindrance still left microscopic defects in the network. Therefore, although the cross-section of ADH3 was notably improved compared with ADH1, the energy dissipation efficiency of the wrinkled structure and the overall density of the network were still intrinsically constrained by the molecular structure of hydrolysable tannins.

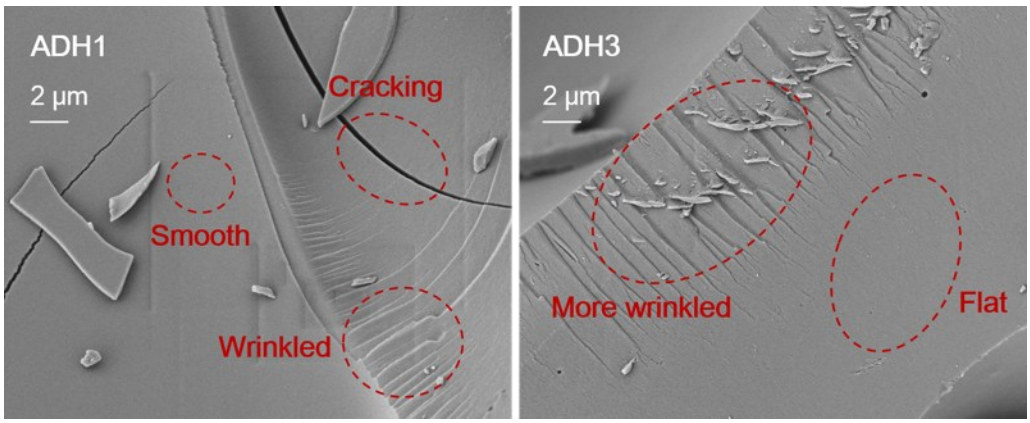

Fig. 3. SEM results of the cross-section of the cured valonia tannin-sucrose adhesive. Note: SEM images of ADH2 were not acquired in the original study. Its microstructural morphology is expected to be intermediate between ADH1 and ADH3.

Thermal Stability Analysis

Taking ADH3 as an example (Fig. 4), the thermal decomposition process of the valonia tannin-sucrose adhesive exhibited obvious multi-stage characteristics, with each weight loss stage corresponding to the pyrolytic behavior of different structural hierarchies, and the overall thermal stability was closely related to the molecular structure of its hydrolysable tannin.

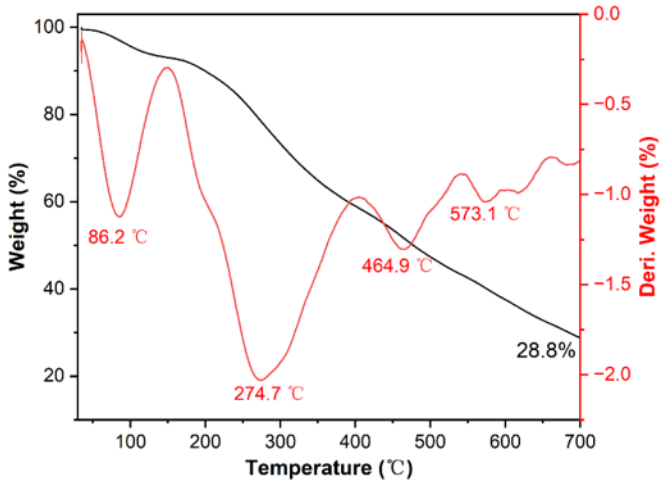

Fig. 4. TG and the derivative results of the cured valonia tannin-sucrose adhesive

In the low-temperature stage, the first thermal decomposition peak appeared near 86.2 °C, which was mainly attributed to the removal of residual moisture and low-molecular-weight volatiles in the adhesive. Because valonia tannin possesses numerous hydrophilic phenolic hydroxyl groups, and because distilled water and small-molecule additives introduced during synthesis were not fully removed by drying, the earliest weight-loss stage was dominated by physical dehydration and the release of low-boiling-point volatiles, resulting in a moderately paced mass reduction.

Entering the medium-temperature stage, $T_{5\%}$ was 107.6 °C, indicating that substantial chemical decomposition of the adhesive began near this temperature. As the temperature continued to rise, $T_{10\%}$ was reached at 199.3 °C, the weight loss rate gradually accelerated, and the maximum weight loss rate peak appeared at 274.7 °C. This stage was the primary interval for the breakage of the most unstable ester bonds in the valonia tannin structure. As a hydrolysable tannin, the gallic acid units of valonia tannin are connected to the central skeleton *via* ester bonds, and the thermal stability of ester bonds is far lower than that of the C-C bond skeleton in condensed tannins (Virtanen *et al*. 2021, 2022; Engström *et al*. 2022). In the 200 to 300 °C range, ester bonds underwent thermal cleavage, galloyl groups detached from the skeleton and further decomposed, releasing small-molecule carboxylic acids, phenols, CO_2, and other volatile products, resulting in rapid mass loss. Simultaneously, the cross-linked network formed by 5-HMF converted from sucrose and the phenolic hydroxyl groups of tannin also began preliminary degradation in this stage, with some ether bonds and hydroxymethyl structures undergoing cleavage. In contrast, condensed tannins, such as bayberry tannin and acacia tannin, whose molecular skeletons are composed of stable C-C bonds, typically exhibit higher main-chain pyrolysis temperatures, slower weight loss rates in the medium-temperature stage, and markedly superior thermal stability compared with valonia tannin systems.

The high-temperature stage was marked by the third thermal decomposition peak at 573.1 °C, corresponding to the deep pyrolysis of the aromatic ring skeleton and further thermal decomposition of the residual char *via* condensation, cleavage, and rearrangement reactions. $T_{30\%}$ reached 317.8 °C, indicating that 30% of the mass loss had been completed by this temperature, with the remaining portion mainly consisting of primary char layers formed during pyrolysis and incompletely decomposed aromatic structures. Near 573.1 °C, the residual aromatic rings underwent condensation, cleavage, and rearrangement reactions, releasing methane, hydrogen, and small amounts of benzene-series volatiles, and

the weight loss rate exhibited another peak. As the temperature continued to rise, the char layer still retained a residual char rate of 28.8% at 700 ℃. Although this residual char rate indicates that the polyphenolic structure of valonia tannin can form a certain amount of char layer through dehydration condensation and aromatization reactions during pyrolysis, it is evidently lower than that of condensed tannin adhesives.

It should be noted that the interpretation of the reaction pathway in this study relies on the mechanistic framework previously established for condensed tannin–sucrose adhesives (Xiao *et al*. 2022, 2023; Liang *et al*. 2025a,b). While the FT-IR, SEM, and TG results presented herein are consistent with 5-HMF-mediated cross-linking, direct confirmation of the specific condensation products between 5-HMF and hydrolysable tannin subunits (*e.g*., galloyl units) by techniques such as solid-state NMR, Py-GC/MS, or model compound reactions was not performed. Therefore, the cross-linking mechanism proposed for the valonia tannin–sucrose system remains a working hypothesis that warrants further fundamental investigation.

CONCLUSIONS

1. The Fourier transform infrared (FT-IR) analysis confirmed that valonia tannin belongs to a typical hydrolysable gallotannin, with ester bond linkages and ortho-trisubstituted benzene ring structures present in the molecule.
2. Increasing the sucrose proportion promoted the generation of 5-HMF during hot pressing. Consistent with the cross-linking mechanism previously validated for condensed tannin–sucrose systems, the aldehyde groups of its furan ring are inferred to form a dense three-dimensional cross-linked network with the phenolic hydroxyl groups of valonia tannin, effectively compensating for the deficiencies of hydrolysable tannins in terms of low reactivity and unstable ester bonds. As the sucrose proportion increased from 66.7% to 100%, the dry strength increased from 1.04 to 1.43 MPa, and the warm-water strength increased from 0.46 to 0.84 MPa, meeting the requirements for Class II plywood specified in the GB/T 17657 (2022) standard.
3. Analysis of the microstructural morphology and thermal stability of the adhesive showed that although the thermal instability of ester bonds resulted in a faster weight loss rate compared with condensed tannin systems, the dense cross-linked network formed at a high sucrose proportion delayed the thermal degradation process to a certain extent and improved the overall thermal stability.
4. This study demonstrated a promising laboratory-scale approach that hydrolysable tannins have long been difficult to utilize in wood adhesives due to their low reactivity and poor thermal stability of ester bonds, providing preliminary experimental support that warrants further investigation under industrially relevant conditions.

ACKNOWLEDGMENTS

This work was supported by the Key Project of Basic Research of Guizhou Province of China (QKHJCZD[2026]021), National Natural Science Foundation of China (32660385, 32160348), and the Outstanding Youth Science and Technology Talent Project of Guizhou Province of China (YQK[2023]003).

REFERENCES CITED

Arias, A., Gonzalez-Garcia, S, Feijoo, G, and Moreira, M. (2021). "Tannin-based bio-adhesives for the wood panel industry as sustainable alternatives to petrochemical resins," *J. Ind. Ecol.* 26(6), 627-642. https://doi.org/10.1111/jiec.13210

Engström, M. T., Virtanen, V., and Salminen, J. P. (2022). "Influence of the hydrolyzable tannin structure on the characteristics of insoluble hydrolyzable tannin–protein complexes," *J. Agric. Food Chem.* 70(41), 13036-13048. https://doi.org/10.1021/acs.jafc.2c01765

GB/T 17657 (2022). "Test methods of evaluating the properties of wood-based panels and surface decorated wood-based panels," Standardization Administration of China, Beijing, China.

Gong, F., Liang, J., Li, C., Yin, S., Yang, G., Lei, H., Yu, L., Li, L., Li, D., Wu, Z., and Du, G. (2026). "The reaction mechanism and performance evaluation of one-pot preparation of full biomass adhesive with defatted soybean and phytic acid," *Ind. Crop. Prod.* 240, article 122639. https://doi.org/10.1016/j.indcrop.2026.122639

Guo, L., Qiang, T., Yang, Y., He, Y., Dou, Y., Zhang, Z., and Wang, H. (2024). "Extraction and structural characterization of hydrolyzable tannins from *Coriaria nepalensis* leaves," *Ind. Crop. Prod.* 215, article 118646. https://doi.org/10.1016/j.inderop.2024.118646

Hou, M., Zhang, Q., Lei, H., Zhou, X., Du, G., Pizzi, A., Essawy, H., and Xi, X. (2025). "Mildew resistant modified starch adhesive by soybean meal flour crosslinking with excellent bonding properties," *Carbohyd. Polym.* 354(4), article 123247. https://doi.org/10.1016/j.carbpol.2025.123247.

Li, D., Cai, B., Wang, Z., Jiang, Q., Ren, C., Wang, J., Wei, Z., Wu, Z., Lei, H. (2025). "Reducing curing temperature of multifunctional sucrose/tannic acid-based wood adhesive *via* catalysis method for improved water resistance and bonding strength," *Chem. Eng. J.* 525, article 170379. https://doi.org/10.1016/j.cej.2025.170379

Li, D., Yu, L., Li, L., Liang, J., Wu, Z., Xu, X., Zhong, X., and Gong, F. (2023). "Melamine-urea-formaldehyde resin adhesive modified with recycling lignin: Preparation, structures and properties," *Forests* 14(8), article 1625. https://doi.org/10.3390/f14081625

Li, J., Lei, H., Xi, X., Li, C., Hou, D., Song, J., and Du, G. (2023). "A sustainable tannin-citric acid wood adhesive with favorable bonding properties and water resistance," *Ind. Crop. Prod.* 201(1), article 116933. https://doi.org/10.1016/j.indcrop.2023.116933

Liang, J., Li, D., Zhong, X., Wu, Z., Cao, M., Yang, G., Yin, S., and Gong, F. (2024). "Crosslinking mechanism of tannin-based adhesives based on model compounds: Copolycondensation of resorcinol with dimethylol urea," *Forests* 15(1), article 98. https://doi.org/10.3390/f15010098

Liang, J., Yang, G., Zhang, M., Lan, L., He, X., Yang, H., Yang, Y., He, Y., Yang, H., and Wu, Z. (2025a). "Morphological remodeling and performance of cured tannin-sucrose adhesive layer: Enhancement by catalyst," *BioResources* 20(4), 10605-10617. https://doi.org/10.15376/biores.20.4.10605-10617

Liang, J., Yin, S., Li, C., Lan, L., He, X., Yang, H., Yang, Y., He, Y., Yang, H., and Wu, Z. (2025b). "Tannin-sucrose adhesive properties: A comparison of bayberry and acacia tannins," *BioResources* 20(4), 10594-10604. https://doi.org/10.15376/biores.20.4.10594-10604

Lin, W. S., and Catchmark, J. M. (2025). "Improved starch adhesives for packaging and wood products," *Polym. Eng. Sci.* 65(4), 1682-1692. https://doi.org/10.1002/pen.27077

Liu, T., Shao, Y., Zhang, X., Wan, J., Du, G., Yang, L., and Ran, X. (2025). "A chitosan-based adhesive with high flame retardancy and superior bonding strength fabricated by interface engineering," *Int. J. Biol. Macromol.* 305(9), article 140984. https://doi.org/10.1016/j.ijbiomac.2025.140984

Ma, L., Peng, H., Wang, X., Chen, L., Mao, S., and Li, Y. (2024). "Surface property enhancement of impregnated paper decorative panel by MUF-polyelectrolyte complex@Nano-Al_2O_3 blending," *Colloid. Surface. A* 691, article 133893. https://doi.org/10.1016/j.colsurfa.2024.133893

Oktay, S., Kizilcan, N., and Bengu, B. (2024). "Environment-friendly cornstarch and tannin-based wood adhesives for interior particleboard production as an alternative to formaldehyde-based wood adhesives," *Pigm. Resin Technol.* 53(2), 173-182. https://doi.org/10.1108/prt-06-2022-0075

Tian, M., Zhang, B., Wu, Z., Yu, L., Li, L., and Xi, X. (2021). "Effects of steam heat-treatment on properties of *Pinus massoniana* wood and its bonding performance," *J. Renew. Mater.* 9(4), 789-801. https://doi.org/10.32604/jrm.2020.013844

Virtanen, V., and Karonen, M. (2020). "Partition coefficients (logP) of hydrolysable tannins," *Molecules* 25(16), article 3691. https://doi.org/10.3390/molecules25163691

Virtanen, V., Green, R. J., and Karonen, M. (2022). "Interactions between hydrolysable tannins and lipid vesicles from *Escherichia coli* with isothermal titration calorimetry," *Molecules* 27(10), article 3204. https://doi.org/10.3390/molecules27103204

Virtanen, V., Räikkönen, S., Puljula, E., and Karonen, M. (2021). "Ellagitannin-lipid interaction by HR-MAS NMR spectroscopy," *Molecules* 26(2), article 373. https://doi.org/10.3390/molecules26020373

Wang, X., Cao, L., Hu, Y., Chen, Y., Jin, T., Huang, J., Zhang, X., and Lin, S. (2023). "Highly transparent, hydrophobic, hard and flexible coatings based on a novel melamine-formaldehyde resin synthesized by hydrophobic melamine," *Prog. Org. Coat.* 179, article 107487. https://doi.org/10.1016/j.porgcoat.2023.107487

Wang, Y., Zheng, X., Jiang, K., Han, D., and Zhang, Q. (2024). "Bio-based melamine formaldehyde resins for flame-retardant polyurethane foams," *Int. J. Biol. Macromol.* 273(Pt 1), article 132836. https://doi.org/10.1016/j.ijbiomac.2024.132836

Wu, Z., Chen, S., Liang, J., Li, L., Xi, X., Deng, X., Zhang, B., and Lei, H. (2021). "Plasma treatment induced chemical changes of alkali lignin to enhance the performances of lignin-phenol-formaldehyde resin adhesive," *J. Renew. Mater.* 9(11), 1959-1972. https://doi.org/10.32604/jrm.2021.016786

Xiao, G., Liang, J., Li, D., Tu, Y., Zhang, B., Gong, F., Gu, W., Tang, M., Ding, X., Wu, Z., and Lei, H. (2022). "Fully bio-based adhesive from tannin and sucrose for plywood manufacturing with high performances," *Materials* 15(24), article 8725. https://doi.org/10.3390/ma15248725

Xiao, G., Liang, J., Wu, Z., Lei, H., Gong, F., Gu, W., Tu, Y., and Li, D. (2023). "A composite whole-biomass tannin-sucrose-soy protein wood adhesive with high performance," *Forests* 14(6), article 1250. https://doi.org/10.3390/f14061250

Yang, G., Liang, J., Li, D., Li, L., Yu, L., Yin, S., Gong, F., Lei, H., Wu, Z., and Du, G. (2026). "A green Schiff base wood adhesive: Tunable strength and toughness *via* oxidized sucrose and aliphatic diamine," *Ind. Crop. Prod.* 245, article 123239. https://doi.org/10.1016/j.indcrop.2026.123239

Zhao, Z., and Umemura, K. (2014). "Investigation of a new natural particleboard adhesive composed of tannin and sucrose," *J. Wood Sci.* 60(4), 269-277. https://doi.org/10.1007/s10086-014-1405-3

Zhao, Z., and Umemura, K. (2015). "Investigation of a new natural particleboard adhesive composed of tannin and sucrose. 2. Effect of pressing temperature and time on board properties, and characterization of adhesive," *BioResources* 10(2), 2444-2460. https://doi.org/10.15376/biores.10.2.2444-2460

Zhao, Z., Sakai, S., Wu, D., Chen, Z., Zhu, N., Gui, C., Zhang, M., Umemura, K., and Yong, Q. (2020). "Investigation of synthesis mechanism, optimal hot-pressing conditions, and curing behavior of sucrose and ammonium dihydrogen phosphate adhesive," *Polymers* 12(1), article 216. https://doi.org/10.3390/polym12010216

Zhao, Z., Umemura, K., and Kanayama, K. (2015). "Effects of the addition of citric acid on tannin-sucrose adhesive and physical properties of the particleboard," *BioResources* 11(1), 1319–1333. https://doi.org/10.15376/biores.11.1.1319-1333

Zheng, G., Zhang, S., Wang, Y., Pan, A., Xu, B., Xu, Y., and Zhang, X. (2025). "Preparation of a multifunctional bio-based adhesive inspired by the structure of dragonfly wings," *Compos. Part B-Eng.* 298(4), article 112374. https://doi.org/10.1016/j.compositesb.2025.112374

Article submitted: July 14, 2026; Peer review completed: August 15, 2026; Revised version received: August 29, 2026; Accepted: August 30, 2026; Published: September 15, 2026.
DOI: 10.15376/biores.21.4.10676-10688